Microscopic mechanism for transient population inversion and optical gain in graphene

Torben Winzer,* Ermin Malić, and Andreas Knorr

Institut für Theoretische Physik, Nichtlineare Optik und Quantenelektronik, Technische Universität Berlin, Hardenbergstraße 36, 10623 Berlin, Germany

(Received 26 July 2012; revised manuscript received 4 December 2012; published 8 April 2013)

Based on microscopic calculations, we predict a transient femtosecond population inversion in graphene suggesting graphene as a new active gain material covering a broad frequency range. In this paper, we microscopically shed light on the underlying elementary many-particle processes: Transient gain and population inversion occur due to an interplay of strong optical pumping and carrier cooling that fills states close to the Dirac point giving rise to a relaxation bottleneck. The subsequent femtosecond decay of the optical gain is mainly driven by Coulomb-induced Auger recombination. Our findings are in excellent agreement with recent experimental data.

DOI: 10.1103/PhysRevB.87.165413 PACS number(s): 78.67.Wj, 73.22.Pr, 78.45.+h, 78.47.jg

Light amplification and optical gain are of central importance in the optical sciences.[1,2] They are based on the quantum effect of induced photon emission and constitute one of the key ingredients in optoelectronic devices and optical data communication.[2] Therefore, there is an ongoing quest for gain materials in different frequency ranges. Particular questions involve the mechanical stability of materials and the possibility of electrical injection. In recent years, much research has been devoted to graphene, a two-dimensional sheet of carbon atoms.[3–6] Besides its distinct transport characteristics,[7] its optical properties have been intensively investigated[5,6,8] with respect to transient broadband[9,10] and saturable[11,12] absorption.

Recently, Li and co-workers[13] also demonstrated the possibility of optical gain based on population inversion in optically pumped graphene within a differential reflection measurement. The experiment reveals that gain appears at pump fluences of approximately 2 $\mathrm{mJ/cm^2}$ on a femtosecond time scale for optical transitions smaller than the pump energy.[13] Graphene as a coherent source of terahertz radiation was first suggested by Ryzhii *et al.*[14] and Satou *et al.*,[15] and experimental indications were recently found in a nondifferential measurement.[16] Due to its unique band structure, graphene has the potential to cover a broad frequency range for light amplification. Since graphene has no band gap and its optical properties are dominated by distinct many-body effects, the observation of optical gain in graphene is crucial to our understanding of the light-matter interaction in this material. In particular, it is of utmost importance for graphene-based applications to understand the conditions for the occurrence of optical gain.

In this article, we perform microscopic calculations on the carrier dynamics in the same excitation regime as recently reported in experiments,[13] confirming the possibility of gain and population inversion in graphene. Our theory goes beyond previous approaches[14,15] by treating the optical pumping and electron-phonon as well as electron-electron scattering on a consistent microscopic footing.[17] Therewith, we develop a complementary understanding with respect to the experiment since our theory directly accesses the time- and momentum-resolved nonequilibrium carrier distribution during and after a strong optical excitation pulse. Therewith, we are able to analyze the predominant interplay of many-body mechanisms and light-matter interaction giving rise to the gain regime. In particular, as the most important result of this paper, we identify as the crucial processes the phonon-induced intraband scattering, which fills optically active states at low energies, and the counteracting Auger recombination. The result of the simultaneous interplay of both processes results in a carrier relaxation bottleneck close to the Dirac point giving rise to a transient population inversion. This specific interplay building up optical gain is, so far, unknown from other materials, and it is remarkable since it occurs phonon induced, despite the presence of strong Coulomb scattering in graphene. The transient decay of the population inversion on a 100-fs time scale can be understood as an efficient interplay of intraband carrier-phonon scattering (energy loss) and Coulomb-induced Auger recombination[18,19] (carrier loss). Signatures of these collinear scattering channels[18] were also recently observed in photocurrent experiments[20,21] and optical pump-probe measurements.[22,23]

Applying the graphene Bloch equations,[17,24] we microscopically consider the light-carrier interaction as well as carrier-carrier and carrier-phonon scattering in a consistent treatment.[25,26] A coupled set of differential equations describes the temporal evolution of: (i) the occupation probability $\rho_{\mathbf{k}}^{\lambda}$ in state $\mathbf{k}$ in the conduction and the valence bands ($\lambda = c,v$), (ii) the microscopic polarization $p_{\mathbf{k}}$ reflecting the transition probability between both bands, and (iii) the phonon occupation $n_{\mathbf{q}}^{j}$ with the momentum $\mathbf{q}$ for different modes j,[17]

$$\begin{aligned}
\dot{\rho}_{\mathbf{k}}^{\lambda} &= 2\,\mathrm{Im}\big[\Omega_{\mathbf{k}}^{\mathrm{vc}*} p_{\mathbf{k}}\big] + \Gamma_{\mathbf{k},\lambda}^{\mathrm{in}}\big[1-\rho_{\mathbf{k}}^{\lambda}\big] - \Gamma_{\mathbf{k},\lambda}^{\mathrm{out}}\rho_{\mathbf{k}}^{\lambda},\\
\dot{p}_{\mathbf{k}} &= \big[i\,\Delta\omega_{\mathbf{k}} - i\Omega_{\mathbf{k}}^{\lambda\lambda} - \gamma_{\mathbf{k}}\big]p_{\mathbf{k}} - i\,\Omega_{\mathbf{k}}^{\mathrm{vc}}\big[\rho_{\mathbf{k}}^{c} - \rho_{\mathbf{k}}^{v}\big] + \mathcal{U}_{\mathbf{k}}, \quad (1)\\
\dot{n}_{\mathbf{q}}^{j} &= -\gamma_{\mathrm{ph}}\big[n_{\mathbf{q}}^{j} - n_{B}^{j}\big] + \Gamma_{j,\mathbf{q}}^{\mathrm{em}}\big[1+n_{\mathbf{q}}^{j}\big] - \Gamma_{j,\mathbf{q}}^{\mathrm{abs}} n_{\mathbf{q}}^{j}.
\end{aligned}$$

The coupling to the exciting pulse is described by the Rabi frequency $\Omega_{\mathbf{k}}^{\mathrm{vc}}$ and its corresponding intraband contribution $\Omega_{\mathbf{k}}^{\lambda\lambda}$. For our analysis, we generate a nonequilibrium carrier distribution via optical excitation, similar to the experimental realization:[13] A laser pulse in $\Omega_{\mathbf{k}}^{\lambda\lambda'}$ with a duration of 10 fs and a photon energy of 1.5 eV is applied. A sketch of excitation and the linear dispersion is shown in Fig. 1(a). A delayed probe pulse (blue) is used to test the pump-induced (red) population change. Many-particle interactions (Γ, $\mathcal{U}_{\mathbf{k}}$, and $\gamma_{\mathbf{k}}$) are treated within second-order Born-Markov approximation where we take into account a self-consistently determined many-particle broadening of the strict energy conservation.[27] We obtain

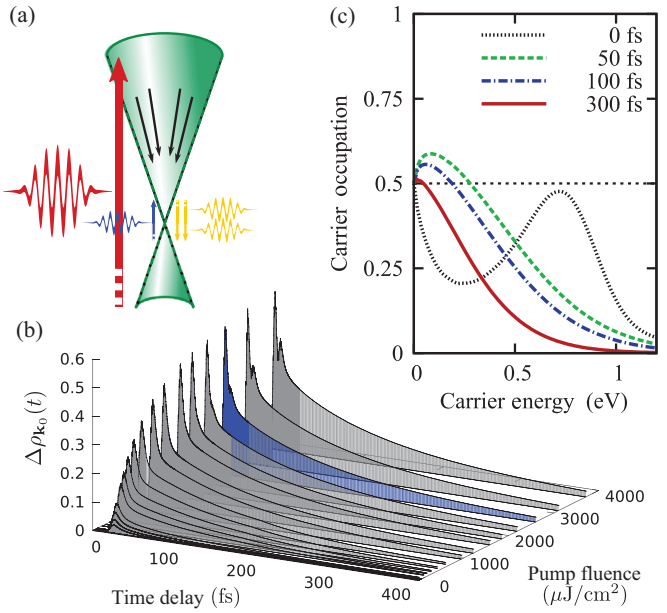

FIG. 1. (Color online) (a) Scheme of optical pumping (red) and the buildup of a phonon bottleneck (black). Energetically lower probe pulse (blue) can be amplified via induced emission (yellow) if population inversion occurs. (b) Pump-induced change in occupation $\Delta\rho_{\mathbf{k}_0}(t)$ in the most efficiently excited state $\mathbf{k}_0$ for different pump fluences. We obtain a qualitatively and quantitatively excellent agreement with the experiment, cf. Fig. 2(b) in Ref. 13. (c) In contrast to the experiment,[13] we have a direct access to the carrier dynamics: Carrier distribution for different delay times after an optical excitation with a pump fluence of approximately 2.5 mJ/cm^2 [marked blue in (b)]. Gain is obtained during the first 300 fs for carrier energies smaller than 250 meV.

a Boltzmann-like scattering equation where the time- and momentum-dependent scattering rates $\Gamma^{\text{in/out}}_{\mathbf{k},\lambda}$ consider carrier-carrier as well as carrier-phonon contributions. A similar equation is obtained for the phonon occupation with the emission and absorption rates $\Gamma^{\text{em/abs}}_{j,\mathbf{q}}$. The microscopic polarization $p_{\mathbf{k}}$ is damped by the many-particle diagonal dephasing $\gamma_{\mathbf{k}}$ and is deformed by the off-diagonal contribution $\mathcal{U}_{\mathbf{k}}$.[17] In exception of the linear transition frequency $\Delta\omega_{\mathbf{k}}$, the experimentally estimated phonon decay rate γ_{ph},[28] and the Bose-Einstein distribution n^j_B as a thermal bath for the dynamic phonon occupation, all terms in Eqs. (1) are explicitly time dependent. A detailed description of these equations can be found in Ref. 17.

For the understanding of the formation of optical gain, we analyze, as an experimentally addressable observable, the pump pulse-induced population inversion $\Delta\rho_{\mathbf{k}}(t)$ at the position of the probe field $|\mathbf{k}_0| = \omega_L/2v_F$, where ω_L is the probe frequency and v_F is the carrier velocity in graphene's linear band structure. From the numerical solution of the graphene Bloch equations (1), we obtain $\Delta\rho_{\mathbf{k}_0}(t)$, which is approximately proportional to the differential optical response, e.g., the reflection $\Delta R/R$.[29,30]

Figure 1(b) shows $\Delta\rho_{\mathbf{k}_0}(t)$ for different pump fluences up to 4 mJ/cm^2. In excellent agreement with the experiment,[13] we observe, in the low-excitation regime, a linear scaling of the peak of $\Delta\rho_{\mathbf{k}_0}(t)$ with the pump fluence and a clearly nonlinear saturation effect in the range of 0.5–1 μJ/cm^2. As a consequence of the ultrashort excitation, we find first signatures of Rabi oscillations at the highest fluence. In agreement with the experiment, this feature disappears for the longer pulse durations used in Ref. 13. The gain (population inversion) regime can be directly observed in the energy-resolved carrier distribution, shown in Fig. 1(c) for an exemplary pump fluence of [marked blue in Fig. 1(b)] at different times after the optical excitation. At time $t = 0$, i.e., at the maximum of the excitation pulse, a peaked nonequilibrium population distribution is found. The low-energy occupation wing stems from the initial thermal distribution at room temperature broadened by relaxation processes already acting during the pulse. In the course of time, after the pulse, the low-energy population increases, and we observe a population inversion for carrier energies of up to 250 meV. An analysis of the distribution shows that, as long as the population inversion is present, no Fermi-Dirac distribution is established. A nonequilibrium between the carrier and the phonon system is present. Depending on the pump fluence, it takes a few hundreds of femtoseconds until equilibrium is reached.

Next, we turn to the microscopic explanation of the formation mechanism of the population inversion. A detailed inspection shows that the population inversion at lower energies is a direct consequence of energy loss of the optically excited carriers due to intraband carrier-phonon scattering, cf. Fig. 2(a) (green, left). This process fills the states with low momenta having a low (linear) density of states. Hereby, the interplay of the reduced density of states (vanishing at $|k| = 0$) and the conserved carrier density results in a higher occupation at lower energies in comparison to the optically excited distribution where no population inversion is found. This process of energy loss within a band is indirectly accelerated by an ultrafast broadening of the nonequilibrium carrier distribution via intraband Coulomb scattering. A counteracting process is the phonon-induced recombination between the bands, cf. Fig. 2(a) (blue, middle). However, in graphene, it is less efficient due to the reduced density of states close to the Dirac point, resulting in a phonon bottleneck.[31]

This overall picture of the population inversion mechanism is supported by Fig. 2. The population distribution 50 fs after the excitation pulse under consideration of different relaxation channels is shown in Fig. 2(b). For the purple line, all scattering channels are considered, and a population inversion is obtained for carrier energies smaller than 250 meV. Next, we neglect carrier-phonon scattering to demonstrate its crucial role for the buildup of a population inversion [blue dashed-dotted line in Fig. 2(b)]. Without this mechanism of intraband energy loss, the population inversion is suppressed by efficient Coulomb-induced Auger recombination,[32–34] sketched in Fig. 2(a) (red). Its redistribution of carriers to higher energies results in a single Fermi distribution for conduction and valence bands with a vanishing chemical potential,[34] cf. Fig. 2(b). Taking into account all relaxation channels but the Auger processes (red dotted line) gives rise to an energetically broad gain regime with an unrealistically extensive persistence. This reflects the role of Auger-induced recombination to the transience of the population inversion.

One direct consequence of the carrier recombination (Auger and electron phonon) in the process of transient population inversion, which is in full agreement with experimental

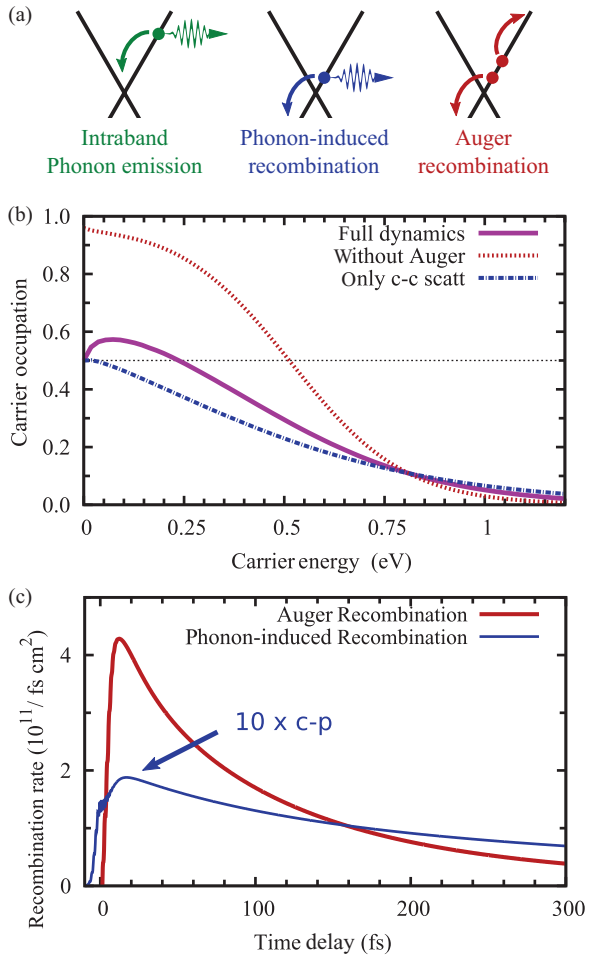

FIG. 2. (Color online) (a) Sketch of the most important scattering channels: energy loss due to intraband phonon emission (green, left), phonon-induced recombination (blue, middle), and Coulomb-induced Auger recombination (red). (b) Carrier distribution 50 fs after the excitation pulse (2.5 μJ/cm^2) considering the full dynamics (purple line), only Coulomb-induced scattering processes (dashed-dotted blue line), and all relaxation channels in exception of Auger processes (dotted red line). The figure illustrates that the intraband carrier-phonon scattering is responsible for the occurrence of the population inversion, whereas, Auger processes are counteracting. (c) Coulomb-induced (red) and phonon-induced (blue) recombination rates, reflecting their contribution to the decay of the gain regime where the process of Auger recombination is the predominant mechanism.

measurements,[13] is a decay of the population inversion on a femtosecond time scale. Such a decay has been measured in the pump-probe signal in Ref. 13. To study the decay of the population inversion in more detail, we analyze the phonon- and Coulomb-induced recombination rates, shown in Fig. 2(c). The rates consider all recombination and carrier-generating processes, including Auger recombination and the counteracting impact excitation. However, in the strong excitation regime, the recombination processes prevails over the hot phonon absorption and impact excitation[34] resulting in an effective carrier loss. Our calculations show that, in this situation, the Coulomb interaction provides the predominant recombination channels (red line) in Fig. 2(c), whereas,

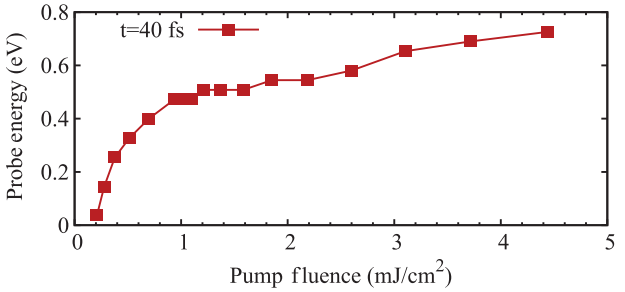

FIG. 3. (Color online) Maximal optical probe energy where a population inversion can be obtained depending on the pump fluence. The values are extracted from the carrier distribution 40 fs after the excitation pulse, corresponding to the temporal resolution of the experiment in Ref. 13.

interband carrier-phonon scattering (blue line) plays a minor role. In particular, immediately after the excitation pulse, the Coulomb-induced Auger recombination reaches values of up to 4×10^{11} fs^{-1} cm^{-2}, which are large compared to the phonon-induced recombination of only 2×10^{10} fs^{-1} cm^{-2} and the overall carrier density of 4×10^{13} cm^{-2}. Consequently, the Auger recombination outweighs the phonon-induced intraband filling of the low-energy states resulting in a femtosecond decay of the population inversion.

A key quest concerning applications of graphene in optoelectronics is the frequency regime where optical gain can be obtained and its dependence on the excitation fluence. As reported in Ref. 13, for a certain excitation strength, the carrier occupation at a probe energy of 1.55 eV remains beneath the gain regime, whereas, at lower probe energies, a population inversion was detected. We use our access to the momentum-resolved carrier distribution to determine the maximal optical probe energy at which population inversion is obtained depending on the pump fluence, shown in Fig. 3.

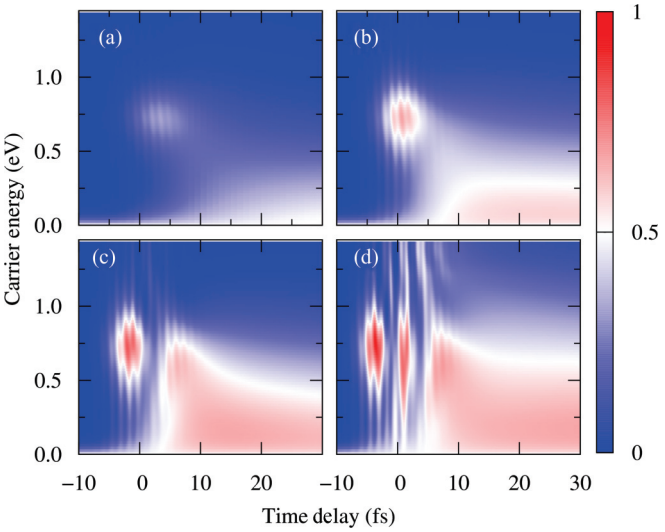

FIG. 4. (Color online) Time- and energy-resolved carrier distributions along the direction of the strongest light-matter coupling during excitations with different pump fluences: (a) moderate excitation regime, (b) gain regime, (c) Rabi-oscillation regime, and (d) second-harmonic regime.

The values are taken 40 fs after the excitation pulse, corresponding to the temporal resolution of the experiment.[13] Up to a critical pump fluence of approximately 200 μJ/cm^2, we observe no population inversion. Above this value, the population inversion appears abruptly at low probe energies. For stronger excitations, the gain regime is broadened up to 0.75 eV. The experimentally observed population inversion at a probe energy of 1.16 eV can be obtained for pump fluences >5 mJ/cm^2. However, our calculations reveal graphene's potential for the amplification of short pulses over a broad energy range since the transient population inversion covers the temporal and spectral ranges of, e.g., a single cycle 50-meV pulse having a duration of 80 fs and a spectral width of 19 meV.

Finally, we analyze the energy-resolved carrier distribution during and after the optical excitation with an increasing pump fluence, cf. Figs. 4(a)–4(d). The shown occupations along the direction of the strongest light-matter coupling in the two-dimensional reciprocal space[17] directly illustrate the action of the exciting laser pulse.[35] The rise of the nonequilibrium occurs wavelike reflecting the optical pump frequency. In exception of panel (a), where a moderate excitation strength beneath the critical value was used, we observe a gain regime (red area) in a broad energy range depending on the applied pump fluence. Note that we also obtain population inversion at the excitation energy decaying on the time scale of the pump pulse duration. However, this should not be visible in experiments using the same temporal resolution for pump and probe pulses. Furthermore, the energy and time resolution of the carrier distribution uncover different aspects of the light-matter coupling in the strong excitation regime. The excitation used in Fig. 4(c) gives rise to Rabi oscillations since optical pumping overweights the diagonal dephasing $\gamma_{\mathbf{k}}$ for the microscopic polarization $p_{\mathbf{k}}$, cf. Eqs. (1). For the highest pump fluence, shown in Fig. 4(d), even a wing of the coherent two-photon absorption is visible.

In conclusion, our calculations confirm the possibility of transient optical gain and population inversion in optically pumped graphene. Despite the presence of strong Coulomb scattering, we identify intraband energy loss via optical phonons as the predominant mechanism for the occurrence of the population inversion. Its decay on a femtosecond time scale is mainly driven by the process of Auger recombination.

We acknowledge financial support from the Deutsche Forschungsgemeinschaft through SPP 1459. E.M. thanks the Einstein Foundation Berlin.

*t.winzer@mailbox.tu-berlin.de

[1] H. Haken, *Laser Theory*, 1st ed. (Springer, Berlin, 1984).
[2] M. O. Scully and M. S. Zubairy, *Quantum Optics* (Cambridge University Press, Cambridge, UK, 1997).
[3] A. K. Geim and K. S. Novoselov, Nat. Mater. **6**, 183 (2007).
[4] A. H. Castro Neto, F. Guinea, N. M. R. Peres, K. S. Novoselov, and A. K. Geim, Rev. Mod. Phys. **81**, 109 (2009).
[5] F. Bonaccorso, Z. Sun, T. Hasan, and A. C. Ferrari, Nat. Photonics **4**, 611 (2010).
[6] P. Avouris and C. Dimitrakopoulos, Mater. Today **15**, 86 (2012).
[7] Y. Zhang, Y. Tan, H. L. Stormer, and P. Kim, Nature (London) **438**, 201 (2005).
[8] D. Sun, C. Divin, J. Rioux, J. E. Sipe, C. Berger, W. A. de Heer, P. N. First, and T. B. Norris, Nano Lett. **10**, 1293 (2010).
[9] K. F. Mak, J. Shan, and T. F. Heinz, Phys. Rev. Lett. **106**, 046401 (2011).
[10] K. F. Mak, L. Ju, F. Wang, and T. F. Heinz, Solid State Commun. **152**, 1341 (2012).
[11] Q. Bao, H. Zhang, Y. Wang, Z. Ni, Y. Yan, Z. X. Shen, K. P. Loh, and D. Y. Tang, Adv. Funct. Mater. **19**, 3077 (2009).
[12] Z. Sun, T. Hasan, F. Torrisi, D. Popa, G. Privitera, F. Wang, F. Bonaccorso, D. M. Basko, and A. C. Ferrari, ACS Nano **4**, 803 (2010).
[13] T. Li, L. Luo, M. Hupalo, J. Zhang, M. C. Tringides, J. Schmalian, and J. Wang, Phys. Rev. Lett. **108**, 167401 (2012).
[14] V. Ryzhii, M. Ryzhii, and T. Otsuji, J. Appl. Phys. **101**, 083114 (2007).
[15] A. Satou, F. T. Vasko, and V. Ryzhii, Phys. Rev. B **78**, 115431 (2008).
[16] S. Boubanga-Tombet, S. Chan, T. Watanabe, A. Satou, V. Ryzhii, and T. Otsuji, Phys. Rev. B **85**, 035443 (2012).
[17] E. Malic, T. Winzer, E. Bobkin, and A. Knorr, Phys. Rev. B **84**, 205406 (2011).
[18] F. Rana, Phys. Rev. B **76**, 155431 (2007).
[19] T. Winzer, A. Knorr, and E. Malic, Nano Lett. **10**, 4839 (2010).
[20] N. M. Gabor, J. C. W. Song, Q. Ma, N. L. Nair, T. Taychatanapat, K. Watanabe, T. Taniguchi, L. S. Levitov, and P. Jarillo-Herrero, Science **334**, 648 (2011).
[21] D. Sun, G. Aivazian, A. M. Jones, J. S. Ross, W. Yao, D. Cobden, and X. Xu, Nat. Nanotechnol. **7**, 114 (2012).
[22] P. A. Obraztsov, M. G. Rybin, A. V. Tyurnina, S. V. Garnov, E. D. Obraztsova, A. N. Obraztsov, and Y. P. Svirko, Nano Lett. **11**, 1540 (2011).
[23] S. Tani, F. Blanchard, and K. Tanaka, Phys. Rev. Lett. **109**, 166603 (2012).
[24] T. Stroucken, J. H. Grönqvist, and S. W. Koch, Phys. Rev. B **84**, 205445 (2011); J. Opt. Soc. Am. B **29**, A86 (2012).
[25] M. Lindberg and S. W. Koch, Phys. Rev. B **38**, 3342 (1988).
[26] F. Rossi and T. Kuhn, Rev. Mod. Phys. **74**, 895 (2002).
[27] J. Schilp, T. Kuhn, and G. Mahler, Phys. Rev. B **50**, 5435 (1994).
[28] K. Kang, D. Abdula, D. G. Cahill, and M. Shim, Phys. Rev. B **81**, 165405 (2010).
[29] M. Breusing, S. Kuehn, T. Winzer, E. Malić, F. Milde, N. Severin, J. P. Rabe, C. Ropers, A. Knorr, and T. Elsaesser, Phys. Rev. B **83**, 153410 (2011).
[30] S. Winnerl, M. Orlita, P. Plochocka, P. Kossacki, M. Potemski, T. Winzer, E. Malic, A. Knorr, M. Sprinkle, C. Berger, W. A. de Heer, H. Schneider, and M. Helm, Phys. Rev. Lett. **107**, 237401 (2011).
[31] S. Butscher, F. Milde, M. Hirtschulz, E. Malić, and A. Knorr, Appl. Phys. Lett. **91**, 203103 (2007).
[32] P. Plochocka, P. Kossacki, A. Golnik, T. Kazimierczuk, C. Berger, W. A. de Heer, and M. Potemski, Phys. Rev. B **80**, 245415 (2009).
[33] R. Kim, V. Perebeinos, and P. Avouris, Phys. Rev. B **84**, 075449 (2011).
[34] T. Winzer and E. Malić, Phys. Rev. B **85**, 241404 (2012).
[35] The results shown in Figs. 1(a), 1(b), and 2(b) stem from angle-averaged carrier distributions.